

## Ultrasonic Embedding of Continuous Carbon Fiber into 3D printed Thermoplastic Parts

Kazi Md Masum Billah<sup>1,2</sup>, Jose L. Coronel Jr.<sup>1,2</sup>, Sarah Chacon<sup>1,2</sup>, Ryan B. Wicker<sup>1,2</sup>, David Espalin<sup>1,2</sup>

<sup>1</sup>Department of Mechanical Engineering, The University of Texas at El Paso, El Paso, TX, USA

<sup>2</sup>W. M. Keck Center for 3D Innovation, The University of Texas at El Paso, El Paso, TX, USA

Corresponding author: kbillah@miners.utep.edu

### Abstract

A novel multimaterial fabrication process was developed to embed continuous bundles of carbon fiber (CF) into polycarbonate (PC) substrates using ultrasonic energy. Continuous CF possesses superior reinforcement properties compared to that of chopped or short fibers. In this research, dry continuous CF bundles were impregnated with a PC solution prior to embedding. Three printing raster orientations were studied (0°, 45°, and 90°), where three layers of CCF were embedded within each test specimen. Characterizations including tensile, flexural, and dynamic mechanical analysis were carried out to investigate reinforcement related properties. Results showed an increase in ultimate tensile strength between neat PC (37 MPa) and CF reinforced specimens (141 MPa). An automated ultrasonic embedding process allowed for the selective deposition of CF, regardless of the raster orientation. Future development of continuous CF reinforced parts could enable smart part fabrication, with applications in structural health monitoring, microwave shielding, and thermal management.

### 1. Introduction

Through the utilization of carbon fiber (CF) reinforced polymer composites, the opportunity for lightweight structure fabrication has attracted a strong interest to the additive manufacturing (AM) community. The capabilities of AM technology, such as complex structure fabrication, selective deposition of materials, and direct fabrication of parts from a design, have enabled the fabrication of composite parts. One of the inherent characteristics of AM technology is the deposition of materials in a layer-by-layer fashion. In the case of thermoplastic material extrusion AM, the inferior mechanical strength of printed parts created the necessity of introducing reinforcing materials such that improved strength could be obtained. In recent years, a significant research effort has been made to create composite materials which improve mechanical strength [1]. Aiming to mechanically reinforce the composites, several forms of fiber materials such as powder, chopped, nanotube, continuous fiber, etc. were added to the thermoplastic matrix materials. Dul *et al.* [2] added graphene nanoparticles (GnP) to ABS thermoplastics to increase the mechanical properties. Although the elastic modulus of the 3D printed GnP reinforced ABS improved with the wt % increase of the nanoparticles, ultimate strength reduced significantly due to the increased viscosity. Ning *et al.* [3] described a method of short CF reinforced ABS filament production and printing. Mechanical characterization results showed that specimens with 5 wt.% short reinforced CF had the largest tensile strength while the further increase of CF i.e. 7.5 wt.% had the highest modulus. Further increase of CF content showed a drastic reduction of the composite strength due to the severity of the porosity. The presence of porosity in the extruded

bead limited the fiber loading fraction. Tekinalp *et al.* [4] also reported the limits of increased CF content and the severe effects of porosity on the extruded beads.

Due to the limitations of short fiber reinforced 3D printed composites, several printing methods have evolved to extrude continuous fibers with thermoplastic materials. Matsuzaki *et al.* [5] reported a method of 3D printing where continuous fiber filaments were extruded using a single nozzle. The key aspect of this printing technique was the impregnation of the fiber within the heated nozzle during printing. Tensile strength and modulus of the jute fiber reinforced PLA composite increased by 435% and 599% respectively. Justo *et al.* [6] characterized long continuous CF reinforced parts which were fabricated using a dual extruder printer MarkOne. The impregnation and compaction of the fibers generated porosity within the printed parts, ultimately reducing the final properties of the composite. To resolve the impregnation issue of the fiber bundles, Li *et al.* [7] utilized the method of fiber preparation before printing. Dynamic mechanical characterization results confirmed the impregnation of the CF bundles within the printed part by enhancing the chain mobility. However, presence of the porosity within the printed parts remained.

This paper describes a method of embedding continuous CF using ultrasonic energy. While the primary goal of this analysis was the reinforcement of the printed part, an earlier investigation showed that continuous carbon fiber embedding into the 3D printed neat polycarbonate (PC) not only enhanced the mechanical properties but also reduced the porosity [8]. This research was conducted in an automated foundry system which allows the users to embed continuous CF bundles in a selective position of the part. Before embedding the CF bundle into the 3D printed

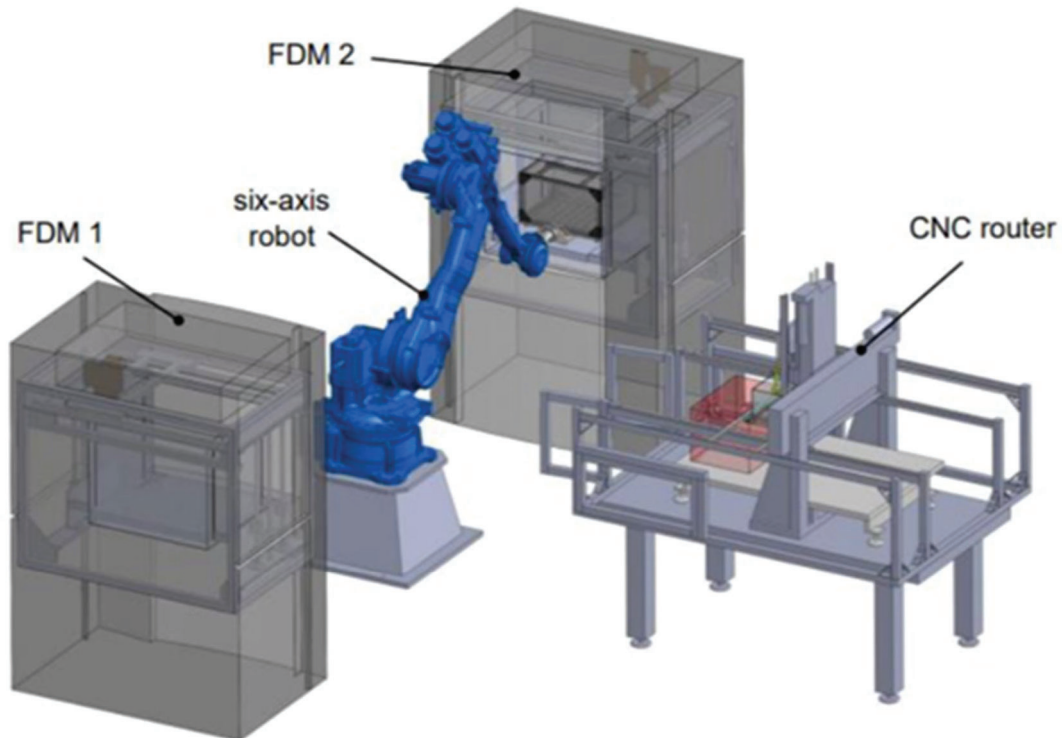


Figure 1. Multi<sup>3D</sup> Foundry System

thermoplastic parts, the impregnation and drying operations were performed. Mechanical characterization was performed on the fabricated specimen. Lastly, this research demonstrated the capability of the foundry system to embed CF in multiple layers of the 3D printed parts.

## 2. Sample fabrication process

A unidirectional continuous carbon fabric (Fibre Glast Developments Corporation, Brookville, OH) was obtained to prepare the CCF. The as-received carbon fiber was non-woven in nature and contained less than 3% of polyester binder so that maximum possible density of CF could be obtained. Considering the dry and weak bonding at the interface between the carbon fibers, surface modification was conducted before embedding the CF in the 3D printed parts. PC pellets harvested from PC filament were mixed (7 wt.% of PC) with a Dimethyl chloride solution. A magnetic stirrer and tip sonicator were used to dissolve the PC pellets for 30 minutes. Using handheld scissors, CFF were cut to have a 7 mm width. To obtain a thick and single sheet type CCF, all the harvested sheets were immersed within the PC solution. Then the CCF sheets were slowly pulled out individually from the PC solution. All the CCF sheets were dried inside a fume hood at room temperature for 5 hours.

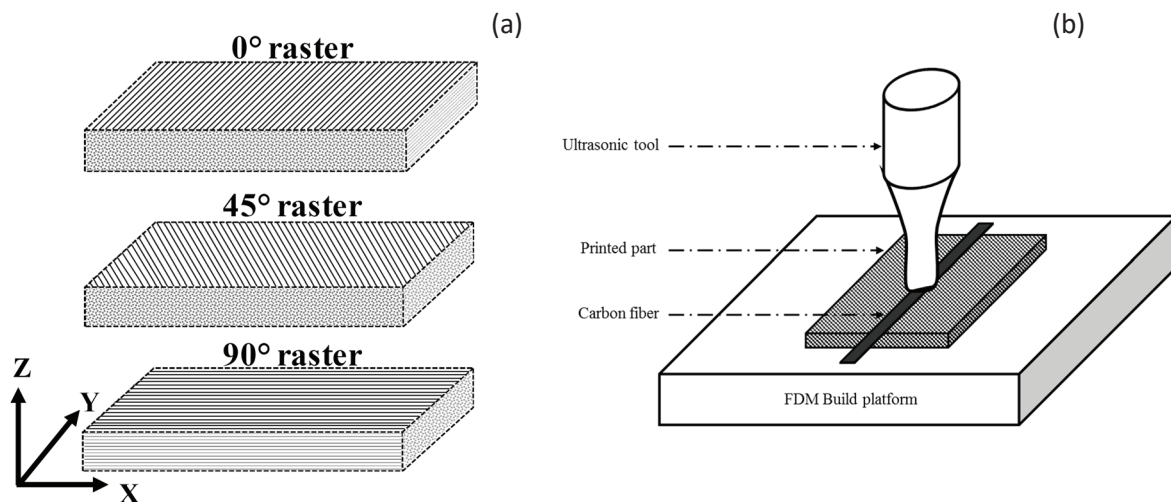


Figure 2. Schematic of raster orientation of 3D printed parts and ultrasonic embedding methods.

Experimental samples were manufactured by a Multi<sup>3D</sup> Foundry System, as shown in Figure 1, consisting of an industrial MH50 six-axis robot (Yaskawa Motoman, Miamisburg, OH, USA) with three manufacturing stations within its reach including two production-grade Fortus 400mc Fused Deposition Modeling (FDM) machines (Stratasys, Eden Prairie, MN, USA) and a LC3024 CNC machine (Techno CNC Systems, Ronkonkoma, NY, USA). The CNC machine is capable of using multiple custom tools, including a wire embedding tool, machining spindle, pick-and-place end-effectors, and a foil application tool as described in [9]–[13]. 3D printed polycarbonate based specimens were fabricated using FDM 400mc machine. For experimental characterization, three different groups of samples were fabricated. ASTM D638 [14] Type-I specimens were fabricated in the XYZ directions with three different raster orientations: (a) 0° (b)



Figure 3. CF embedded ASTM D638 Type-I specimens

45°, and (c) 90° as shown in 2(a). Printing parameters were as follows: layer thickness 0.25 mm, printing temperature 368 °C, and T16 tips were used for support and model materials.

Using the program controlled “Pause and Go” options, printing was paused after the 6<sup>th</sup> layer out of a total of 13 layers. A continuous CF sheet was embedded in the middle of the total 13 i.e. after 6<sup>th</sup> layer pause was inserted. After inserting the pause mechanism in the printing process, the FDM build platform was transferred to the CNC router where the CCF embedding

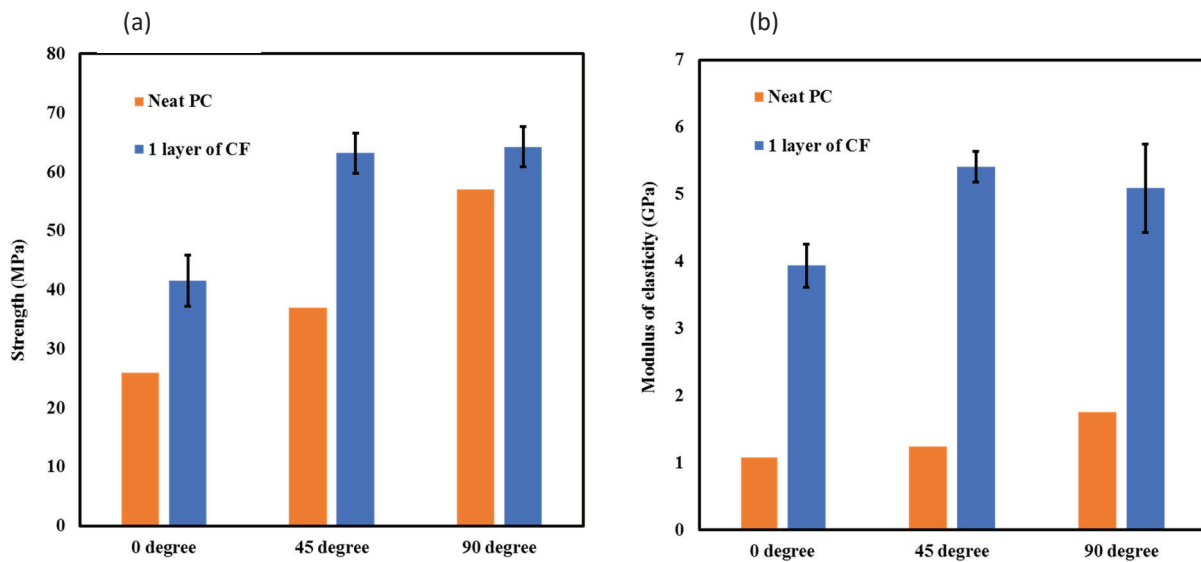


Figure 4. Schematic of raster orientation of 3D printed parts and ultrasonic embedding

process was performed. The schematic procedure of ultrasonic embedding is shown in 2(b). Note that, mechanical properties of the neat PC were studied in the past, thus authors conducted experiment on five CF embedded specimens and one neat specimen as shown in Figure 3.

### 3. Result

The results of the tensile strength tests for the three different raster angles are presented in Figure 4. For all cases, the UTS increased compared to the neat specimen. Figure 4(a) shows the tensile strengths of CF embedded specimens with three different raster orientations. In the cases of 45° and 90° RA, similar tensile strengths were obtained although there was a difference in fracture strains (1.6% and 1.8% respectively). At the beginning of each test the tensile curve exhibited lower strength and slope of curves than the follow-up test stages. This was due to the clamping force between the PC specimen and the test clamps of the tensile testing machine. In the elastic region, there was a slight change in slope due to the debonding of the fiber matrix interface. Similar behavior was demonstrated for PLA and impregnated CF printing in [N. Li. *et al.* 2016]. All cases defined the yield point and when the fracture occurred, beyond the elastic region.

The UTS comparison between different RA's and neat specimens showed that in the case of 0° RA, the strength increased by 60% due to CF embedding. The highest percentage increase in UTS achieved in 45° RA was 70% (~38 MPa to ~68 MPa) compared to the neat specimen. Although it was hypothesized that 90° RA would have higher strength compared to rest of the RA, the embedding process limited the strength due to the breakage of printed beads on the edge of the tensile specimen. The UTS of the 90° RA was increased by 13% compared to the neat specimen. The comparison between the modulus of the neat and CF embedded specimens showed a significant improvement in 45° RA. The neat PC modulus increased by ~233 % for 0 ° RA, ~267 % for 45° RA, and 177 % for 90° RA.

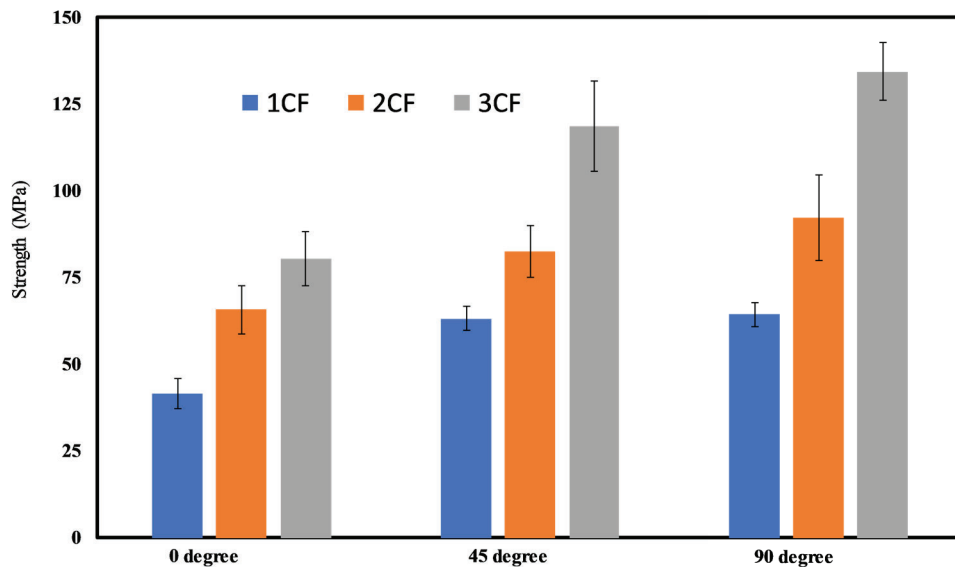


Figure 5. Comparison of ultimate strength of multilayer CF specimen

To demonstrate the capability of multilayer embedding using the foundry system with an ultrasonic apparatus, two and three layers of CF were embedded into printed specimens. In the case of two layer CF specimens, the fiber bundles were embedded in the 5<sup>th</sup> and 9<sup>th</sup> layers. Three layers of CF embedding occurred in the 4<sup>th</sup>, 7<sup>th</sup> and 10<sup>th</sup> layers of the specimen. Figure 5 represents the ultimate strength comparisons between one, two, and three layers of CF embedded specimens. As the number of CF layers increased within the printed part, the strength also increased substantially. However, there was a limitation on the dimensional stability of the multiple layer CF embedded specimen. The mismatch of the coefficient of thermal expansion between CF and PC resulted in dimensional inaccuracy which was confirmed by Naim et al. [8]. Although dimensional inaccuracy is a limiting factor of embedding CF in neat plastic materials, authors envisioned that future thermal environments could potentially eliminate the issue of warping.

#### 4. Conclusion

This research described a novel method of CF embedding technology using ultrasonic energy. Mechanical reinforcement of plastic materials was achieved by introducing a fraction of CF bundles in selective layers. In the context of digital manufacturing, the entire printing and embedding processes were done in the Multi<sup>3D</sup> Foundry System, with the exception of the CF sheet preparation. Results of different RA showed the maximum strength obtained was in 45° RA i.e. 70% of tensile strength increased compared to the neat specimen and the modulus increased by 267%. While the automated ultrasonic embedding process allowed the user to deposit CF bundles in selective layers, the enhancement of dimensional stability becomes critical when introducing large volume fractions of CF bundles. Authors envision future research to conduct flexural testing to assess the laminar strength of CF and PC materials. Also, a basic demonstration of potential structural health monitoring will be performed to determine the applicability of CF not only for reinforcing, but also to be used as a sensor.

#### References

- [1] Wang, X., Jiang, M., Zhou, Z., Gou, J., and Hui, D. (2017). 3D printing of polymer matrix composites: A review and prospective. *Composites Part B: Engineering*, 110, 442-458.
- [2] Dul, S., Fambri, L., and Pegoretti, A. (2016). Fused deposition modelling with ABS-graphene nanocomposites. *Compos. Part A Appl. Sci. Manuf.*, 85, 181-191.
- [3] Ning, F., Cong, W., Qiu, J., Wei, J., and Wang, S. (2015). Additive manufacturing of carbon fiber reinforced thermoplastic composites using fused deposition modeling. *Compos. Part B Eng.*, 80, 369-378..
- [4] Tekinalp, H. L., Kunc, V., Velez-Garcia, G.M., Duty, C.E., Love, L. J., Naskar A. K., Blue, C. A., and Ozcan, S. (2014). Highly oriented carbon fiber-polymer composites via additive manufacturing. *Composites Science and Technology*, 105, 144-150.
- [5] Matsuzaki, R., Ueda, M., Namiki, M., Jeong, T. K., Asahara, H., Horiguchi, K., Taishi, N., Todokori, A., & Hirano, Y. (2016). Three-dimensional printing of continuous-fiber composites by in-nozzle impregnation. *Scientific reports*, 6, 1-7, 20.

- [6] Justo, J., Távora, L., García-Guzmán, L., & París, F. (2018). Characterization of 3D printed long fibre reinforced composites. *Composite Structures*, 185, 537-548.
- [7] Li, N., Li, Y., & Liu, S. (2016). Rapid prototyping of continuous carbon fiber reinforced polylactic acid composites by 3D printing. *Journal of Materials Processing Technology*, 238, 218-225.
- [8] Jahangir, M. N., Billah, K. M. M., Lin, Y., Roberson, D. A., Wicker, R. B., & Espalin, D. (2019). Reinforcement of material extrusion 3D printed polycarbonate using continuous carbon fiber. *Additive Manufacturing*, 28, 354-364.
- [9] Ambriz, S., Coronel, J., Zinniel, B., Schloesser, R., Kim, C., Perez, M., ... & Wicker, R. B. (2017). Material handling and registration for an additive manufacturing-based hybrid system. *Journal of Manufacturing Systems*, 45, 17-27.
- [10] MacDonald, E., Espalin, D., Doyle, D., Muñoz, J., Ambriz, S., Coronel, J., ... & Wicker, R. (2018). Fabricating patch antennas within complex dielectric structures through multi-process 3D printing. *Journal of Manufacturing Processes*, 34, 197-203.
- [11] Billah, K. M. M., Coronel, J. L., Halbig, M. C., Wicker, R. B., & Espalin, D. (2019). Electrical and Thermal Characterization of 3D Printed Thermoplastic Parts With Embedded Wires for High Current-Carrying Applications. *IEEE Access*, 7, 18799-18810..
- [12] Coronel Jr, J. L., Fehr, K. H., Kelly, D. D., Espalin, D., & Wicker, R. B. (2017, May). Increasing component functionality via multi-process additive manufacturing. In *Micro- and Nanotechnology Sensors, Systems, and Applications IX* (Vol. 10194, p. 101941F). International Society for Optics and Photonics.
- [13] K. M. M. Billah, J. Luis, C. Jr, R. B. Wicker, and D. Espalin, "Effect of porosity on electrical insulation and heat dissipation of fused deposition modeling parts containing embedded wires," 29<sup>th</sup> Solid Freeform Fabrication Symposium An Additive Manufacturing Conference, Austin, TX, 2018.
- [14] ASTM International. (2015). *ASTM D638-14, Standard Test Method for Tensile Properties of Plastics*. West Conshohocken, PA.